Weather Situation-Dependent Stratification of Precipitation and Upper-air Verification of the Alpine Model (aLMo)

Andrea M. Rossa, Marco Arpagaus, and Emanuele Zala

MeteoSwiss, Krähbühlstrasse 58, 8044 Zurich, Switzerland

Abstract

A weather situation-dependent verification of the Alpine Model's (aLMo) quantitative precipitation forecasts (QPFs) is presented making use of the Schüepp weather classification and composited quantitative precipitation estimates (QPEs) as observed by the Swiss Radar Network (SRN). The aim of this study is to identify weather situation-dependent QPF strengths and weaknesses of the aLMo, with particular focus on two important forecasting regions, one on the northern and one on the southern side of the Alps.

For the two climatic years 2001 and 2002, i.e. 1 December 2000 to 30 November 2002, the well known overall wet bias of the aLMo has been confirmed and regionalized. A significant dependency of the aLMo QPF performance on the weather situations emerges and is documented. For the two classes 'high' and 'low' the QPF error differences are set in relation to errors in other model variables as detected in the aLMo upper-air verification. Moreover, the aLMo QPF quality for the forecasting region on the southern side of the Alps is found to be significantly lower than for the northern Alpine region.

1 Introduction

The limitations of monthly, seasonally, and yearly statistical verifications of numerical weather prediction (NWP) models are well known, in that their performance is judged over the whole spectrum of weather types the atmosphere can produce. The danger herewith is that it can mask differences in forecast quality when the data, even in terms of flow regimes, are not homogeneous. Further, it can bias the results toward the most commonly sampled regime (for example days with no severe weather). Stratifying the samples into specific subsets (e.g. relative to geographical regions, intensity of observations, or flow regimes) helps to identify forecast behaviour for these particular subsets. A weather situation-dependent classification can help to construct such a stratification.

Since 1945 the Alpine Weather Statistics (AWS) has been available for the central European Alps. Its 34 parameters are defined on a daily bases by the Swiss National Weather Service, MeteoSwiss, on using a set of objective criteria. A thorough description of the AWS can be found in German in Schüepp (1979) and a somewhat more synthesized one in English in Wanner et al. (1998). Parameter 33 of the AWS denotes the daily weather classification after the Schüepp system into 40 classes, commonly referred to as the Schüepp Wetterlageneinteilung.

Present-day operational NWP models' mesh sizes allow for the resolution of meso-β-scale flow phenomena not adequately resolved by traditional observing networks based on surface and upper-air stations. On the other hand, meteorological radars offer precipitation estimates with high spatial and temporal resolution thus providing a means for judging the model's simulated mesoscale structures in the quantitative precipitation forecast (QPF) fields. Radars are not widely used for NWP model verification. Goeber and Milton (2002) have presented verification analyses of the UK Met Office's mesoscale model with their radar

network to document the areal performance of the model's QPFs. Also, coordinated efforts are underway in COST-717's ('use of radar observations in hydrological and NWP models', see e.g. Rossa 2000) WG-2 to enhance exploitation of radar data in this area.

In this report results are presented of a 24 months stratified verification of the Alpine Model's (aLMo) precipitation fields against the Swiss Radar Network (SRN) precipitation estimates and the aLMo's vertical profiles against radio soundings. The stratification is performed using the Schüepp classification. In section 2 the data set, including the weather classification is described, and in section 3 the results are discussed. In the concluding section 4 a summary and a short outlook is given.

2 Data sets and methodology

2.1 Alpine Weather Statistics (AWS)

The Alpine Weather Statistics (AWS) introduced by Schüepp (Schüepp 1979, Wanner et al. 1998) constitutes a set of 34 parameters describing many atmospheric phenomena. Five out of these, namely geostrophic surface wind direction (D, Par. 9), wind speed at 500 hPa (f, Par. 11), wind direction at 500 hPa (d, Par. 10), geopotential height at 500 hPa (hh, Par. 17), and baroclinicity (b, Par. 14) are synthesized into the so-called Schüepp Wetterlageneinteilung (Par. 33). The Schüepp classification scheme consists of 40 different weather classes which describe the synoptic situation at 12 UTC on a daily basis with a geographical focus on the Alpine region (defined by a circular area with radius $\approx$ 220 km centred at Rheinwaldhorn in south-eastern Switzerland) and is available since 1945.

For the purpose of this study, the 40 classes according to Schüepp have been grouped into 9 larger classes, roughly separating the different weather situations into:

- four advective classes *'west'*, *'north'*, *'east'*, and *'south'*, characterized by appreciable surface winds and westerly, northerly, easterly, and southerly winds at 500 hPa, respectively;
- three convective classes *'high'*, *'flat'*, and *'low'*, classified by weak surface winds and above normal, average, and below normal geopotential height on 500 hPa;
- a *'jet'* class featuring strong winds on 500 hPa;
- and a *'mix'* class.

For the time period 1 December 2000 to 30 November 2002 the separation into the different classes is given in Table 1. Particular attention has to be given to gathering large enough samples to give trustworthy verification results, i.e. interpretation of verification results for classes 'east' and 'mix' is limited.

2.2 Radar

Estimating surface rain rates from radar observations, especially in complex terrain, is a challenging task (e.g. Meischner et al. 1997). Being a remote sensing system and measuring only backscattered electromagnetic signals, the derivation of QPEs at the ground suffers from a number of problems, notably: ground clutter, partial beam blocking resulting in areas with low visibility, bright band effects, anomalous propagation, beam attenuation (especially for long ranges and cases of intense precipitation), and side lobe or second trip echoes. Considerable effort has been — and continues to be — put into overcoming some

	AWS code / sub-classes	DJF	MAM	JJA	SON	total
west	+Wp, –Wp, +Wx, –Wx	12	10	10	8	**40**
north	+Np, –Np, +Nx, –Nx	16	19	19	26	**80**
east	+Ep, –Ep, +Ex, –Ex	8	5	0	1	**14**
south	+Sp, –Sp, +Sx, –Sx	17	11	6	14	**48**
high	H0, Hw, Hn, He, Hs	34	29	44	21	**128**
flat	F0, Fw, Fn, Fe, Fs	36	64	80	73	**253**
low	L0, Lw, Ln, Le, Ls	7	15	12	7	**41**
jet	Wj, Nj, Ej, Sj, +Xj, –Xj	46	25	11	27	**109**
mix	Xx, +X0, –X0	4	6	2	5	**17**
adv	west, north, east, south	53	45	25	49	**182**
conv	high, flat, low	77	108	136	101	**422**
all	adv, conv, jet, mix	180	184	184	182	**730**

Table 1: Number of days for each of the nine combined Schüepp classes 'west', 'north', 'east', 'south', 'high', 'flat', 'low', 'jet', and 'mix' and the super-classes 'adv', 'conv', and 'all' for the climatic years 2001 and 2002 (1 December 2000 to 30 November 2002).

of these problems. Nevertheless, radar measurements provide high quality rain/no rain information within the range of the radar site with high spatial and temporal resolution. Quantitatively, however, the SRN QPEs need to be handled with care.

The Swiss Radar Network (SRN) consists of three C-band Doppler radars of the same type, located on Mt. Albis (close to Zurich), Mt. La Dole (close to Geneva), Mt. Lema (close to Lugano), providing full volume information every five minutes (e.g. Joss et al. 1998 and Germann and Joss 2003 for details). The data are pre-processed and available on a cartesian grid with a mesh size of $1 * 1 * 1\,\mathrm{km}^3$ for single radar sites and $2 * 2 * 2\,\mathrm{km}^3$ for the network composite. For the present study best estimates of surface precipitation are used to which a number of state-of-the-art corrections have been applied, including clutter elimination and vertical profile correction algorithms. Overall, the radar product used ('RAIN') is known to systematically underestimate precipitation[1], where the underestimation is strongly dependent on the visibility of the radar. Figure 1 depicts the visibility of the SRN composite in terms of the geometrical height of the lowest pixel the SRN can see at a given location. The blind spots in the regions of Valais and Engadin and the scarce visibility along the main Alpine crest indicate where most care must be exercised in the interpretation of the radar precipitation estimates.

To circumvent the difficulties related to the comparison of the highly variable precipitation fields only 24 hour accumulations are considered for this study. The SRN QPE accumulations are taken from 06 UTC to 06 UTC of the consecutive day and, for the purpose of comparison, were aggregated and interpolated onto the aLMo grid. The aLMo QPFs are taken from the daily operational 00 UTC integration for the forecast range +06 h to +30 h. The overall period spans the two climatic years 2001 and 2002, i.e. 1 December 2000 to 30 November 2002, whereby for the present study only days in which rain has been detected by the Swiss raingauge network[2] were used, i.e. 571 out of the 730 days.

[1] efforts are underway to correct for this bias

[2] for a rain day 5 of the $\approx$ 450 gauges were required to report at least 0.5 mm/24 h

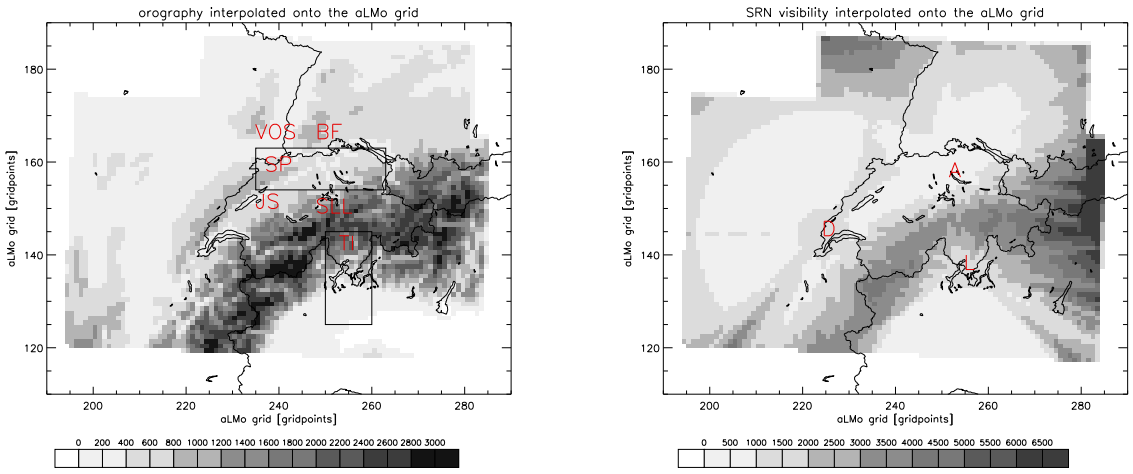

Figure 1: Orography (left panel) and visibility (right panel) for the Swiss Radar Network (SRN) domain interpolated onto the Alpine Model (aLMo) grid in meters above mean sea level. The visibility denotes the height of the lowermost pixel seen by the SRN at a given location. Values below 2000 m allow for good radar performance, while values above 4000 m give only poor precipitation estimates. On the left panel a number of areas referred to in the discussion are delineated, on the right panel the locations of the three radars of the SRN, where 'A' stands for the 'Albis', 'D' for the 'Dole', and 'L' for the 'Lema' radar.

'BF'	Northern Switzerland and Black Forest
'VOS'	Vosges
'SP'	Swiss Plateau
'JS'	Southern slopes of Jura
'SLL'	South of Lake of Lucerne
'TI'	Ticino region in southern Switzerland

Table 2: Definition of regions used for discussion of the precipitation analysis. See Fig. 1 for the geographical locations of these regions.

2.3 Upper-air verification

The vertical structure of the Alpine Model is verified against radiosonde measurements. Observations from 28 stations distributed over the entire aLMo integration domain and delivering upper-air information every twelve hours, i.e. at 00 UTC and at 12 UTC, are used. The parameters verified are geopotential height, temperature, relative humidity, wind direction, and wind speed. The observed data are compared with model variables on a prescribed number of pressure levels (e.g. 750 hPa, 700 hPa, 650 hPa). The observations available for the pressure levels in question (i.e. 'standard TEMP levels', e.g. 700 hPa) are directly used for the verification. For other levels (e.g. 750 hPa and 650 hPa) they are obtained by interpolation of data available on neighbouring pressure levels. The aLMo data are always interpolated to the required pressure levels.

3 Discussion of results

In section 3.1 an overview of the SRN QPEs, the aLMo QPFs, and the aLMo upper-air verification is given. Section 3.2 contains the definition and description of conspicuous features found in the precipitation difference climatology, while in section 3.3 its weather situation dependency is discussed. In section 3.4 the aLMo QPF error differences are set in relation to

errors in other model variables as detected in the aLMo upper-air verification. Sections 3.5 and 3.6 provide a summary on the mean QPF performance on two important forecasting regions respectively for all Schüepp classes and different precipitation intensities.

3.1 Overview on the two year climatology

3.1.1 Radar precipitation estimates

The two year accumulation of the SRN QPE, shown in Fig. 2, needs to be studied with some care and in conjunction with the SRN visibility map (Fig. 1). The maxima in north-eastern and southern Switzerland correspond well with the long-term precipitation climatology (Schwarb et al. 2001, not shown), as well as a minor maximum over and on the eastern flank of the Black Forest. West of it, over the Vosges ('VOS'), however, the SRN climatology does not exhibit the precipitation maximum reported by Schwarb et al. (2001). Moreover, the dry band along the Alpine crest is well described by the SRN, although these lower values may be affected by the radar's scarce visibility over much of the higher portions of the orography.

A major weakness of the SRN is found over western Switzerland and neighbouring France. While the long-term climatology clearly shows local precipitation maxima over the French Jura and the Haute Savoy the SRN reports a rather uniform field of low values. As a matter of fact, the La Dole radar had major hardware problems that caused several data gaps and enhanced systematic underestimation during the period under consideration. In this region comparison with the aLMo is not quantitatively reliable.

Finally, there are two non-meteorological features towards the southern border of the SRN domain linked to non-eliminated ground clutter on the French-Italian Alps, and an (illegal) microwave emitter in the Po Valley. These structures are excluded from the discussion.

3.1.2 aLMo precipitation fields

The gross structure of the aLMo climatology does look surprisingly realistic when compared to the Schwarb et al. (2001) climatology, in that it successfully reproduces the maxima in central, north-eastern, and southern Switzerland. Also, the dry band along the Alpine crest is present. However, precipitation is substantially overestimated, a factor of two or more when compared to the radar.

3.1.3 Upper-air verification

The vertical structure of the Alpine Model is verified operationally using radio soundings launched twice daily (00 and 12 UTC) from 28 stations distributed all over Europe. Amongst other features visible on the verification plots, the most noteworthy results are the systematic warm bias in the upper half of the troposphere and the negative mean error for wind speed throughout most of the troposphere, both increasing with increasing forecast time. The detailed report of the operational verification can be found in section ??? of this newsletter.

Figure 3 depicts the mean error (BIAS) and the standard deviation (STD) of temperature for forecast time +48 h and classes 'conv', 'adv', 'mix', and 'jet' for the climatic years 2001 and 2002 averaged over a set of six stations close to the Alps. A large cold bias can be observed for the 'jet' class, which may be due to a systematic bias of the driving global model GME (for more on this topic, see the report "Upper-air verification at MeteoSwiss for 2002: Highlights" on page ??? of this newsletter). As to the classes 'conv' and 'adv', the mean temperature bias for both classes is fairly similar throughout the troposphere and the larger standard deviation for the advective class as compared to the convective class may be attributed to larger flow-dependent uncertainty of individual forecasts for advective situations.

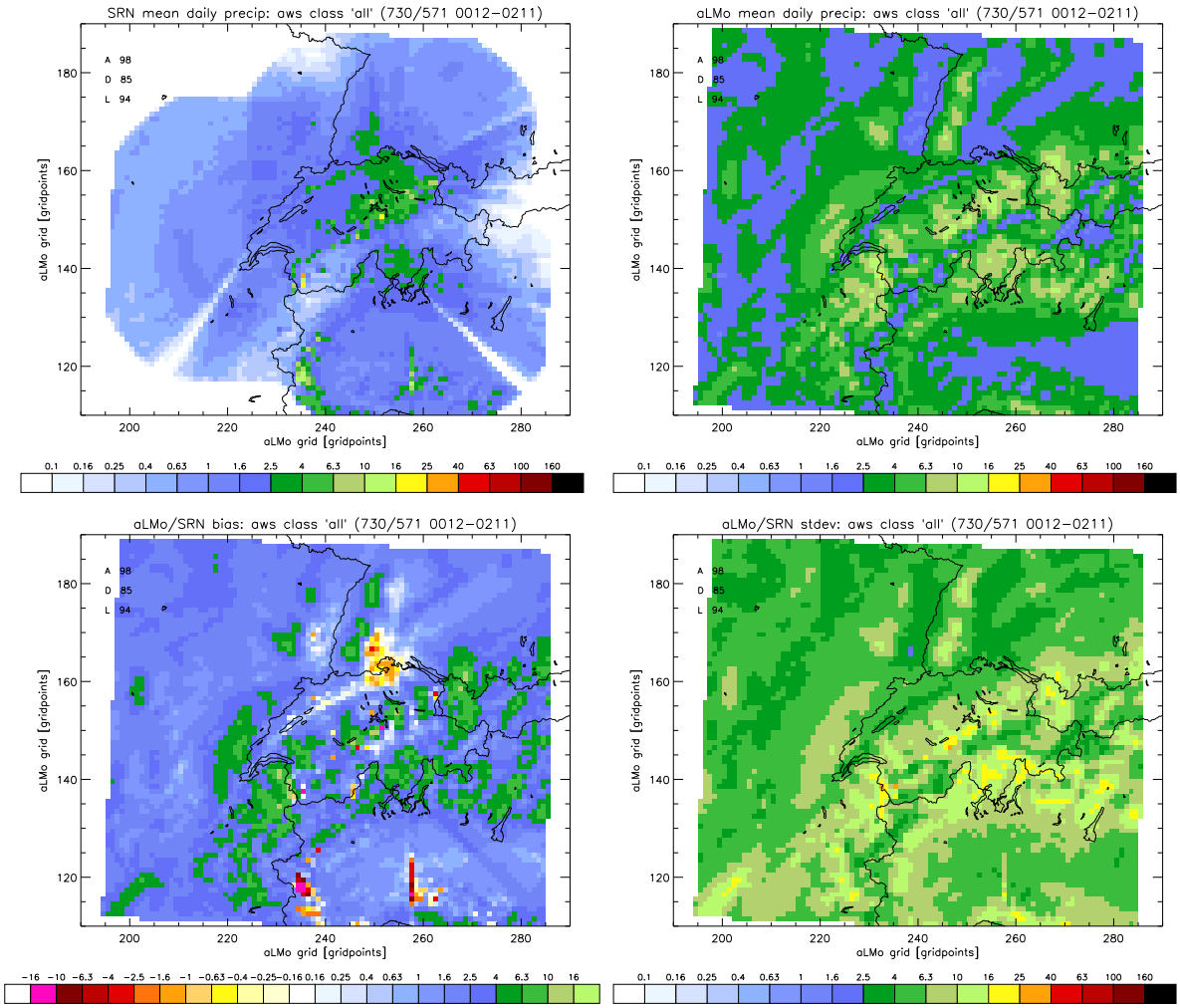

Figure 2: Precipitation comparison between the Swiss Radar Network (SRN) and the Alpine Model (aLMo) for all rain days in the two climatic years 2001 and 2002 (1 December 2000 to 30 November 2002), i.e. 571 of 730 days. Upper left and right panels denote the mean SRN precipitation estimates and the corresponding mean aLMo precipitation forecasts, respectively, while the bias and the standard deviation are shown in the left and right lower panels, respectively. The units of all plots are mm/24 h, the scale is logarithmic. The small numbers in the upper left corners of the plots denote the availability in % of the three radars of the SRN, where 'A' stands for the 'Albis', 'D' for the 'Dole', and 'L' for the 'Lema' radar.

3.2 Description of conspicuous features in the precipitation error climatology

The lower panels of Fig. 2 depict the bias and standard deviation of the aLMo QPFs relative to the SRN QPEs for the entire period. Again, it is obvious from the bias that the aLMo amply overdoes the precipitation on most of the SRN domain by 3 mm/24 h on average, and locally up to 10 mm/24 h. Also, that the error variability as measured by the standard deviation is largest in areas of large precipitation featuring widespread values of 5–10 mm/24 h. For the purpose of this analysis, however, we will concentrate on the bias field keeping in mind the large variability. As a matter of fact, it exhibits a number of conspicuous mesoscale features which will be described in the following, with reference to Fig. 1 and Table 2.

The most prominent structure is a dry bias of the order of 1 mm/24 h with locally larger values in northern Switzerland and neighbouring Germany, east of the Black Forest ('BF'),

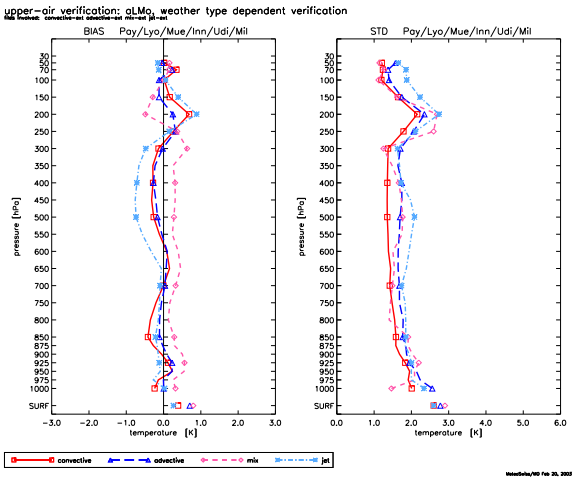

Figure 3: Verification (mean error (BIAS) and standard deviation (STD)) of temperature for classes 'conv' (solid red), 'adv' (dashed blue), 'mix'(dashed magenta), and 'jet' (dash-dotted cyan) for forecast time +48 h and the climatic years 2001 and 2002 (1 December 2000 to 30 November 2002; averaged over Alpine sounding stations in Payerne, Lyon, Munich, Innsbruck, Udine, and Milano; 12 UTC verification time).

with a distinct wet bias juxtaposed to the west. This dipole, actually a double penalty, results from a systematically wrong positioning of the precipitation by the aLMo on the peaks of Black Forest in the model orography with too little of it on the eastern slopes. A similar pattern, albeit less pronounced, is evident in connection with the Vosges ('VOS').

There are two regions where the aLMo produces precipitation amounts that actually compare quite well with the radar values, i.e. the southern slopes of the Jura ('JS') and a region in central Switzerland, just south of the Lake of Lucerne ('SLL'). Taking into account the overall precipitation excess in the aLMo forecasts, however, these regions still may be considered as relatively dry in the model.

On the other hand, the aLMo features a distinct wet bias in the Ticino region ('TI') in southern Switzerland, where the SRN is reliable. More positive peaks in the bias can be seen in a sequence lining up from along the northern solpes and peaks of the Alps all across Switzerland, separated by areas of a lesser wet bias. Unfortunately, the western and eastern-most portions of this structure are not reliably covered by the SRN during the period under consideration.

3.3 Weather situation-dependency of model errors

In this section the weather situation-dependency of the aLMo QPF errors is documented for classes 'conv' and 'adv' in section 3.3.1, for 'jet' in 3.3.2, for 'north' and 'south' in 3.3.3, and 'east' and 'west' in 3.3.4. Weather classes 'high' and 'low' are discussed and related to errors in other model variables as detected in the upper-air verification in section 3.4.

3.3.1 Convective ('conv') versus advective ('adv') weather situations

A first and gross stratification between weather types can be done by distinguishing convective ('conv') and advective ('adv') weather situations (see Table 1 for statistics). Figure 4 displays the aLMo QPF biases for these two classes. Essentially, they exhibit the same features identified for the overall data set ('all'), except that for 'conv' the amplitude of the bias is somewhat smaller than for 'adv' and 'all'. Particularly, the relatively dry bias in the region south of the Lake of Lucerne 'SLL' region is present in 'conv' but only to a lesser degree in 'adv'.

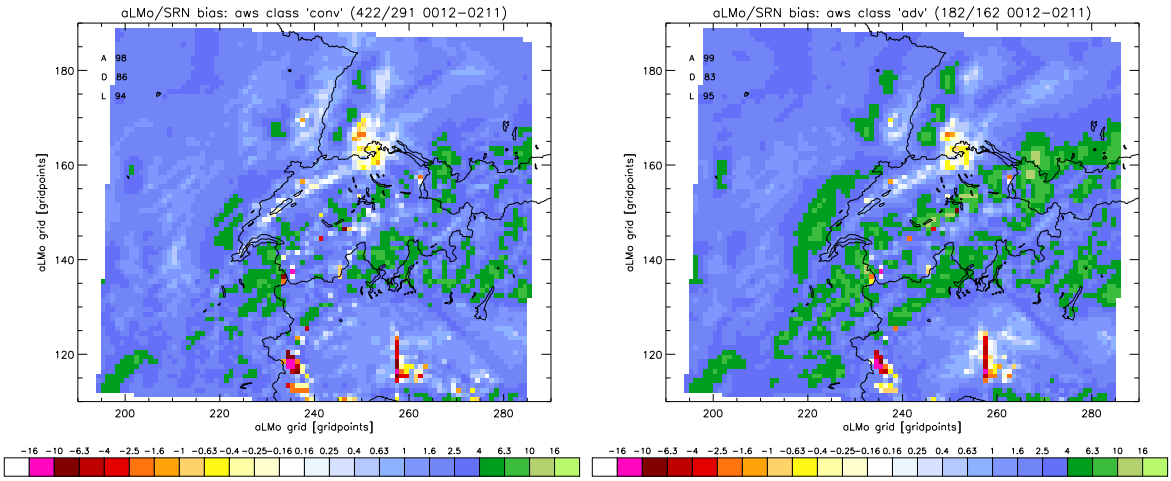

Figure 4: Biases of the aLMo precipitation forecast relative to the SRN estimates for the weather classes 'conv' (left panel) and 'adv' (right panel) for all rain days in the two climatic years 2001 and 2002 (1 December 2000 to 30 November 2002), i.e. 291 of 422 days for 'conv', and 162 of 182 days for 'adv'. The units are mm/24 h, the scale is a logarithmic one ranging from −16 to +16 mm/24 h. The small numbers in the upper left corners of the plots denote the availability in % of the three radars of the SRN, where 'A' stands for the 'Albis', 'D' for the 'Dole', and 'L' for the 'Lema' radar.

3.3.2 Dynamic weather situations ('jet')

The class of 'jet' weather situations is characterized by particularly dynamic flow situations. Again, the bias chart for 'jet' shows the same features as in 'all', which for this case with much more pronounced. The 'BF' structure now exhibits a widespread dry bias of the order of 5 mm/24 h extending into the region 'JS' with values of 0.6 mm/24 h. The above mentioned sequence of stronger and weaker wet biases is accentuated into a succession of wet and dry biases in an area of reasonable radar credibility. The wet biases attain values of 10 mm/24 h and more over relatively large regions, while the dry biases are indicative for 'blind or dry spots' of the aLMo in strong wind situations. Moreover, the precipitation maximum in the 'TI' region seems to be shifted upslope to the northeast, as indicated in the bias. However, the maximum bias is located in a region where the SRN visibility is rather poor.

3.3.3 Weather situations of northerly and southerly flow ('north' and 'south')

The overall orientation of the Alpine range makes the weather situations of northerly ('north') and southerly ('south') flow of special interest, particularly with respect to precipitation. Figure 6 displays the QPF bias fields for these two classes. For 'north' the features discussed for 'all' that are located north of the Alps are retained, except for a larger amplitude of the wet bias anomalies on the northern slopes. On the southern side of the Alps, however, there is a sharp gradient in the region south of the Lake of Lucerne ('SLL'), indicating that the aLMo is not able to produce enough precipitation on the upper part of the lee slope. Half a dozen gridpoints downslope there is a moderate wet bias, whereas even more downwind in the region of the Lago Maggiore and southward into the Po Valley there is again a larger dry bias. The 71 days involved in this analysis should provide a large enough sample to document this systematic underestimation of the aLMo precipitation even over larger distances on the southern side of the Alps in northerly flow situations.

During southerly flow the model behaves somewhat congruently. Indeed, there is a large wet bias on the windward side featuring the position of the maximum at the right location, but not its amplitude. The crest again constitutes a firm barrier for model precipitation resulting

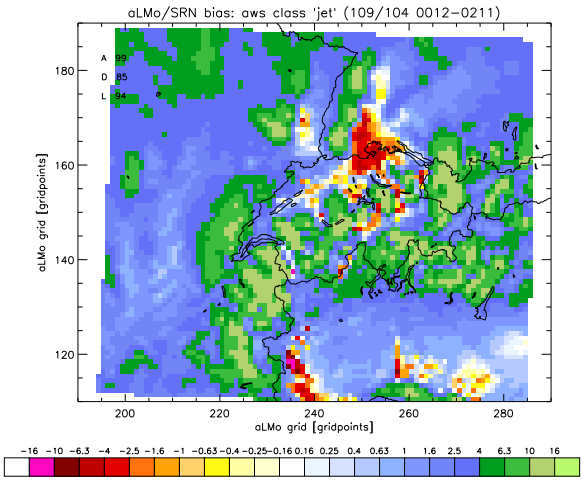

Figure 5: As in figure 4 but for weather situation 'jet' (104 of 109 days detected as rain days).

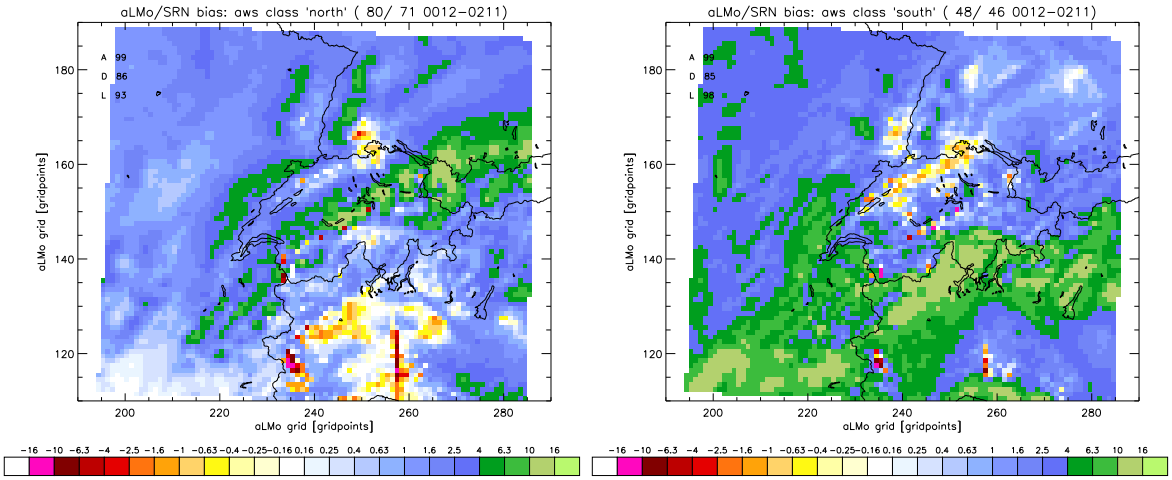

Figure 6: As in figure 4 but for weather situations 'north' and 'south' (71 of 80 and 46 of 48 days detected as rain days, respectively).

in relatively low biases on the northern side of the Alps extending way into southern Germany, and distinct dry biases over large portions of the Swiss Plateau ('SP').

Some of these features may be explained by the model's inability to transport precipitating water and ice. The current grid-scale precipitation scheme (Doms and Schättler 1999) deposits any excess moisture in the same grid-box where saturation occurs. This results in overestimation of precipitation on the windward side of the orography and a pronounced underestimation of precipitation on the lee side of any orographic obstacle (see e.g. Damrath 2002). A prognostic precipitation scheme recently implemented into the Alpine Model (Doms et al. 2001) includes horizontal and vertical advection of hydro-meteors and may alleviate or even eliminate some of the problems described above.

3.3.4 More weather situation dependent forecast errors

A behaviour of the aLMo QPF related to the one found for classes 'north' and 'south' can be documented in the three smaller classes of easterly ('east') and westerly ('west') flow, and

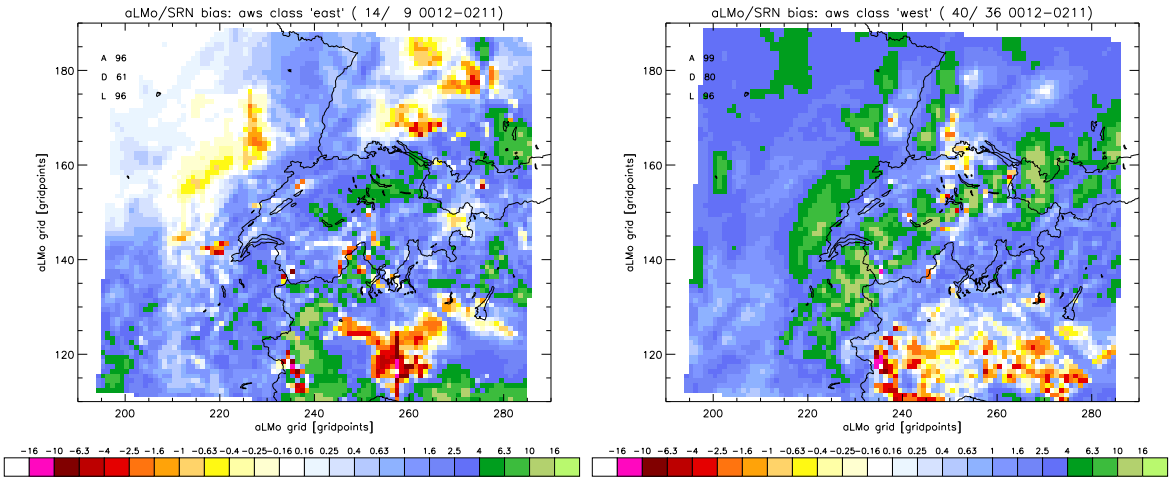

Figure 7: As in figure 4 but for weather situations 'east' and 'west' (9 of 14 and 36 of 40 days detected as rain days, respectively).

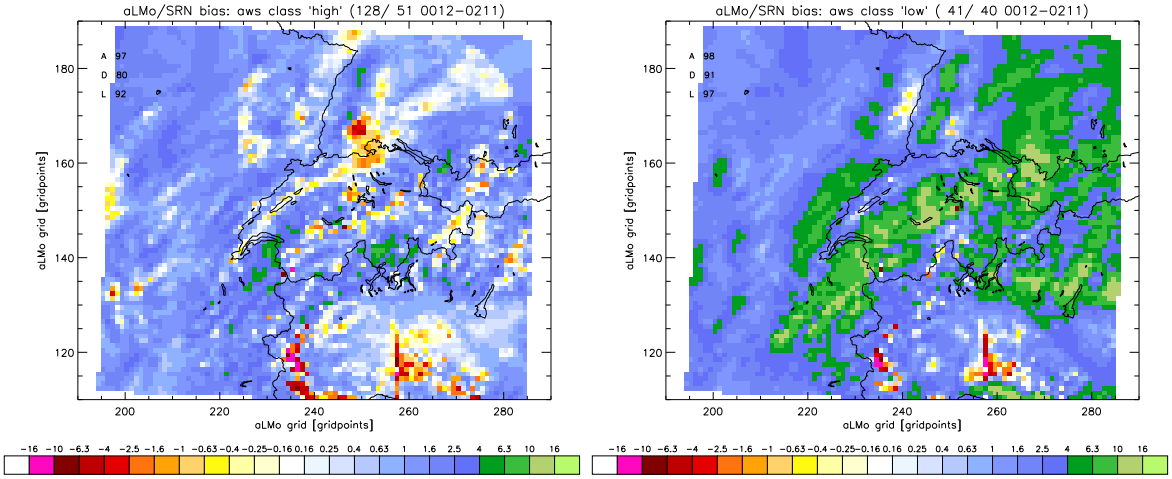

Figure 8: As in figure 4 but for weather situations 'high' and 'low' (51 of 128 and 40 of 41 days detected as rain days, respectively).

mixed ('mix', not shown) weather situations, in that for all three classes there is a distinct dry bias in the plains of the Po Valley. For 'east' there is a wet bias on the eastern slopes of the French-Italian Alps. The aLMo precipitation field (not shown) indeed features a large precipitation maximum on these slopes. Apparently, the aLMo is not able to release enough precipitation on the Po Valley but transports most of it straight onto the mountain slopes. However, the 9 rainy days for 'east' may not be a large enough sample to provide systematic evidence.

3.4 Link of QPF errors to errors in other model variables

'High' and 'low' weather situations are predominantly characterised by dry, fair weather and rainy weather, respectively. The aLMo QPFs perform very differently for these two classes in that the mean bias (Fig. 8) shows a quite dramatic overestimation of precipitation for weather situation 'low' featuring widespread values of the order of +10 mm/24 h and a mean areal bias of 4.5 mm/24 h, in contrast to a much smaller, although positive, mean areal bias of 1.5 mm/24 h for the class 'high'.

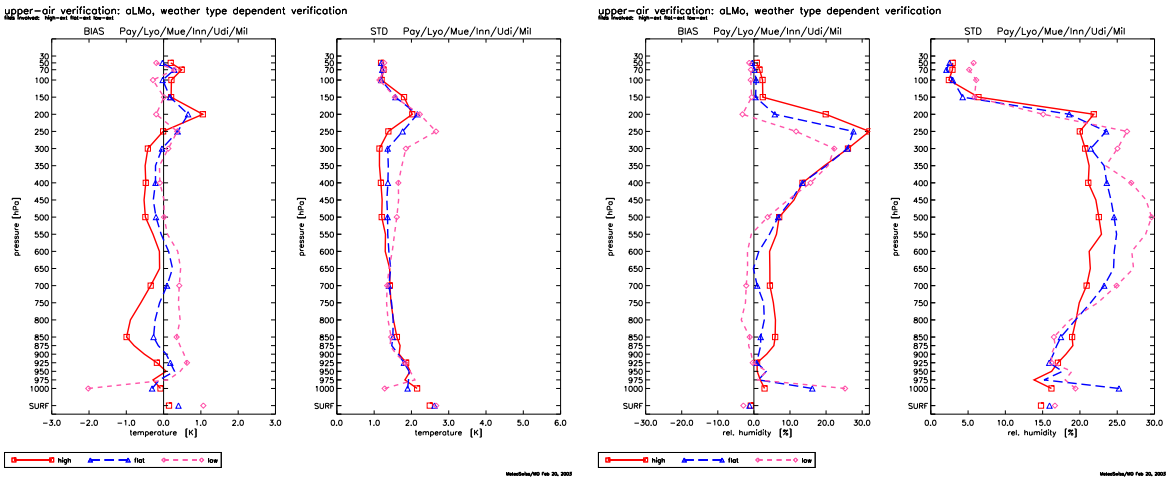

Figure 9: Verification (mean error and standard deviation) of temperature and relative humidity for convective classes 'high' (solid red), 'flat' (blue), and 'low' (dashed magenta) for forecast time +48 h and the climatic years 2001 and 2002 (1 December 2000 to 30 November 2002; averaged over Alpine sounding stations in Payerne, Lyon, Munich, Innsbruck, Udine, and Milano; 12 UTC verification time).

In order to investigate the effects of such large bias differences on other model variables, we look at temperature and humidity profile biases and standard deviations shown in Fig. 9 for classes 'high' and 'low' at forecast time +48 h. A clear warm bias throughout the lower half of the troposphere is evident for class 'low' as well as a significant cold bias up to the tropopause for class 'high', both of which are not present at analysis time (not shown). Concerning relative humidity, 'low' features a dry bias whereas 'high' shows a moist bias in a substantial portion of the troposphere[3], again both not present at analysis time (not shown). The biases seen for relative humidity could be interpreted in terms of the temperature biases, the explanation of the latter being unclear. However, referring to the large differences in the precipitation biases for classes 'high' and 'low', another interpretation is possible: The warm and dry biases documented for weather situations 'low' are consistent with the model's tendency to overestimate moist diabatic processes for this class, therefore excessively heating and drying the model atmosphere! For class 'high', the interpretation is not as straightforward. The precipitation bias for this class (Fig. 8, left panel) shows that the overestimation by the aLMo is much less evident than for class 'low', typically less than 2.5 mm/24 h. Indeed, there are even some pronounced areas of clear underestimation. The fact that the temperature bias for 'high' still is negative and relatively large, despite the present overestimation of precipitation, is consistent with a distinct, although smaller, global negative temperature bias in the model, which in turn may be caused by the driving model (see section 3.1.3). As above, the bias in relative humidity would again be a consequence of the temperature error.

A simple estimate for the difference in latent heating throughout the troposphere[4] caused by the 3 mm/24 h excess precipitation for 'low' relative to 'high' yields a temperature difference on the order of:

$$\Delta T = \frac{\Delta m_{\mathrm{precip}} L}{m_{\mathrm{air}} c_p} = \frac{3\ \frac{\mathrm{kg}}{\mathrm{m}^2}\ 2.5 \cdot 10^6\ \frac{\mathrm{J}}{\mathrm{kg}}}{6 \cdot 10^3\ \mathrm{kg}\ 10^3\ \frac{\mathrm{J}}{\mathrm{kg\,K}}} \approx 1.25\,\mathrm{K}.$$

[3] neglect the bias of relative humidity above $\approx$ 700 hPa due to artificially increased moisture values at analysis time to compensate for the inability of the model to handle saturation with respect to ice

[4] we assume heating up to 8 km in an atmosphere with a scale height of 10 km resulting in roughly $6 \cdot 10^3$ kg of air to be heated

This is in surprisingly good agreement with the temperature bias differences between classes 'high' and 'low' (Fig. 9).

3.5 Weather situation-dependent QPF performance for two important forecasting regions in Switzerland

Figure 10 shows a summary for the precipitation comparison over all the weather classes for the two areas 'Swiss Plateau' (left panel), an important forecasting area on the northern side of the Alps, and 'Ticino' (right panel), dito for the southern side of the Alps (see Fig. 1 for definition). Looking at the areal mean biases and standard deviations normalized with the areal mean SRN precipitation (referred to as bias and standard deviation for convenience sake in this context) the following observations can be made for the region 'Swiss Plateau':

- classes 'east' and 'mix' have anomalously high error values but are not discussed here because of their small sample size;
- classes 'low', 'north', and to a lesser degree 'west' stand out in terms of large biases, 'low' and 'north' are the only classes with biases larger than one, i.e. the aLMo appears to have most difficulties during weather that falls into these classes characterized by rainy weather;
- classes 'high', 'flat', 'south', and 'jet' exhibit a bias of the order of 30 % down to 20 % of the bias of class 'low', i.e. significantly smaller, while the respective standard deviations are in the order of 60–40 % of the value for 'low', except for 'high' which reaches to roughly 80 %;
- class 'jet', although afflicted by large regional biases (see Fig. 5) and characterized by substantial amounts of precipitation, seems to be relatively well predictable for this region;
- class 'adv' is characterized by a 50 % larger bias when compared to 'conv', but a slightly smaller standard deviation, which may reflect a more systematic behaviour of the aLMo in advective situations.

The corresponding error analysis for the 'Ticino' area on the southern side of the Alps looks rather different. In comparison to the 'Swiss Plateau' the 'Ticino' region is characterized by:

- generally substantially larger errors, both in terms of bias and standard deviation, especially for 'all', where the relative bias is about three times as large for 'TI'; forecaster experience confirms the difficulties related to QPFs for the southern side of the Alps;
- 'low' and 'north' are the only classes with a bias equal or smaller than one, whereby 'north' is to be considered carefully because of very little rain in the 'TI' region;
- classes 'south' and 'low', the two classes with most abundant precipitation, have smallest standard deviation, i.e. forecast variability; class 'jet' has a bias similar to 'south' but a standard deviation that is almost twice as large.

3.6 Precipitation intensity-dependency of the QPF error

In this section we briefly discuss the dependency of the QPF performance on precipitation intensity. The upper panels of Fig. 11 show the QPF bias for areal mean precipitation intensity 1.0 mm/24 h (left panel) and 4.0 mm/24 h (right panel). For the lower threshold

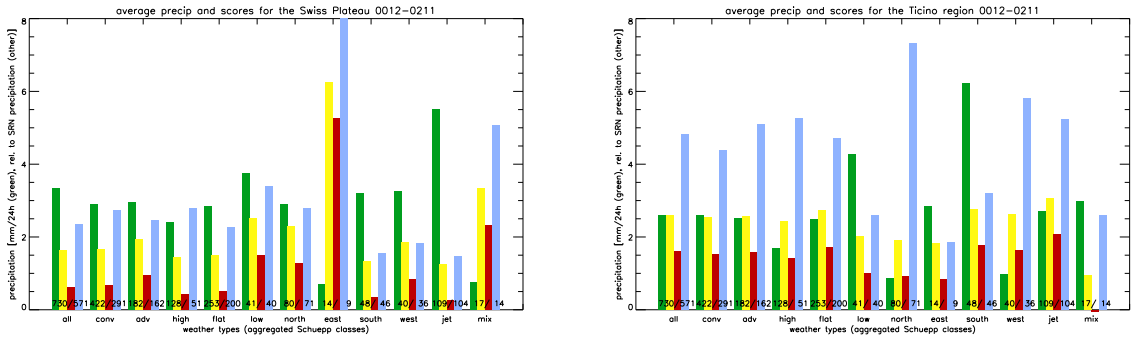

Figure 10: Summary of the aLMo-SRN precipitation comparison for areas 'Swiss Plateau' (left panel) and 'Ticino' (right panel, see Fig. 1 for definition) for the period 1 December 2000 to 30 November 2002. The columns denote respectively the areal mean SRN precipitation (green) in mm/24 h, aLMO (yellow) precipitation, bias (red), and standard deviation (blue) relative to the mean SRN precipitation, for all weather classes as defined in Table 1. The numbers at the bottom of the columns indicate the number of days/rain days for the respective class. Note that the value of the clipped column standard deviation for 'east' and 'Swiss Plateau' is 13.1.

value about half of the rain days of the period under consideration are retained, whereas the higher value is more selective retaining only 27 days. For the 1.0 mm/24 h threshold the structure of the bias field looks very similar to the one for class 'all' (Fig. 2) except for significantly enhanced amplitudes, both for the wet and the dry regions.

For the 4.0 mm/24 h threshold, on the other hand, new features in the bias field emerge. On the wet side, a large region of bias values larger than 10 mm/24 h is visible much along the southern flank of the Alps. This is in line with the fact that many of the 27 members in this selection exhibit strong precipitation in the south. The enhanced dry bias just north of the Alpine crest ('SLL') again points to the aLMo's weakness in properly distributing precipitation across a topographic barrier. This effect is reproduced for the Appenines and the Po Valley, and, on a much smaller scale in the Valtellina Valley, east of Lago di Como. The weakening of the dry spot in the Black Forest region ('BF') is linked to the south-westerly to southerly cases of this sample for which the aLMo places large amounts of rain in this area, which appears to be shun in terms of precipitation by the model in most of the other flow regimes.

A quite large and obvious region of dry bias emerges west of the Jura mountains over relatively flat terrain with a large wet band juxtaposed to the east of it over the Jura. Looking at the single days of this sample this dry region is the result of cases in which the aLMo misplaces frontal precipitation areas, and therefore is a manifestation of the double penalty problem. In an incident of north-westerly flow the aLMo placed the precipitation maximum over the French Jura where the SRN reported the maximum some ten gridpoints upstream. Apparently, the aLMo was not able to trigger the release of precipitation over the relatively flat terrain.

Finally, the summary bar charts for different precipitation intensities show that the relative error of the aLMo QPFs systematically decreases with increasing threshold for both regions considered. Again, the 'TI' region exhibits a much larger error than the 'SP' region.

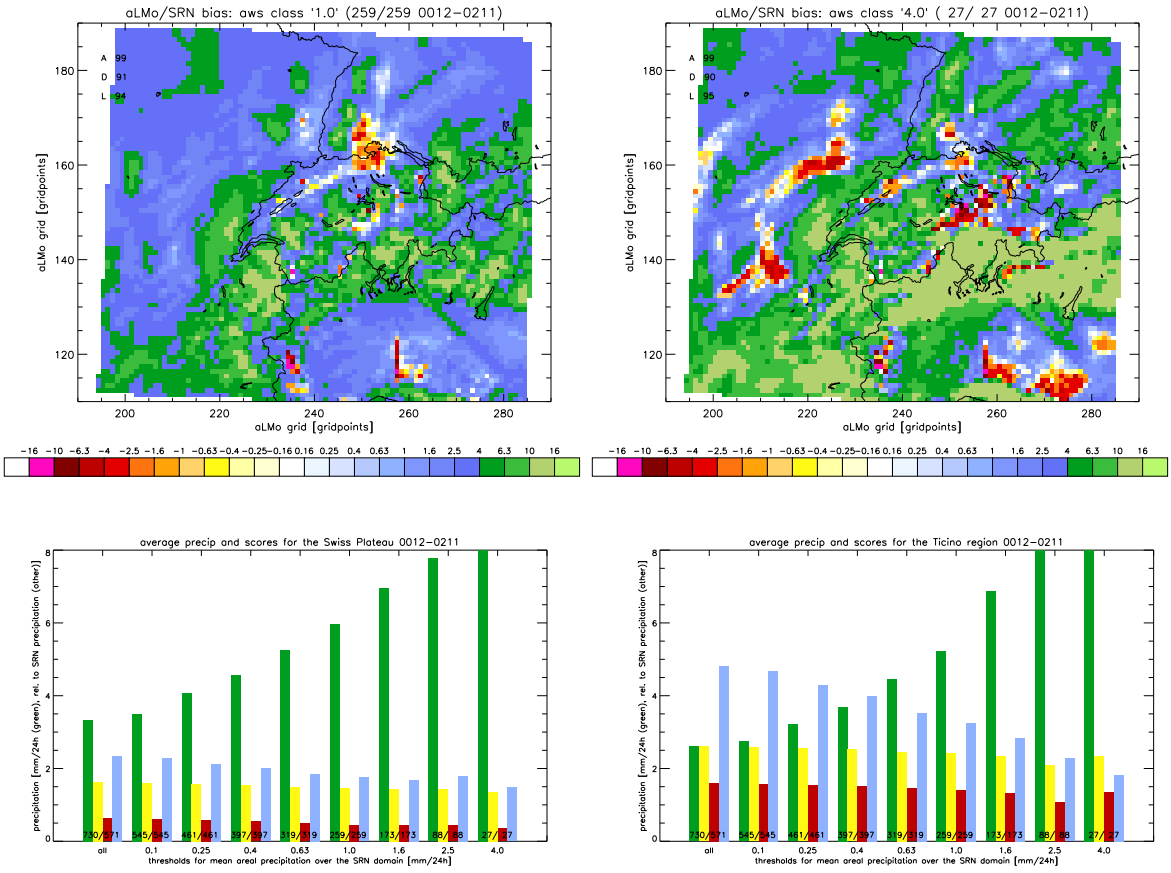

Figure 11: Upper panels as in Fig. 4 but for areal mean precipitation intensities larger than 1.0 mm/24 h (left panel) and 4.0 mm/24 h (right panel). The mean is taken over the entire SRN domain (see Fig. 1). Lower panels as in Fig. 10 but for mean precipitation intensities larger than 0.1, 0.25, 0.4, 0.63, 1.0, 1.6, 2.5, and 4.0 mm/24 h for the regions 'Swiss Plateau' (left panel) and 'Ticino' (right panel, see Fig. 1 for definition). All panels are evaluated for the period 1 December 2000 to 30 November 2002. Note that the value of the clipped column SRN QPE for threshold 4.0 and region 'Swiss Plateau' (left panel) is 10.7, while for thresholds 2.5 and 4.0 and region 'Ticino' 10.5 and 15.5, respectively.

4 Summary

A systematic weather situation-dependent comparison of quantitative precipitation forecasts (QPFs) of the Alpine Model (aLMo) with the quantitative precipitation estimates (QPEs) of the Swiss Radar Network (SRN) has been presented for the two climatic years 2001 and 2002, i.e. 1 December 2000 to 30 November 2002. Overall, the approach is able to produce weather situation-specific statements regarding the aLMo QPF performance. It pinpoints a number of characteristic weaknesses, and is, therefore, worthwhile being pursued. In summary the analysis yielded:

- significant differences of aLMo QPF for different weather classes;
- confirmation of the aLMo QPF overestimation and documentation of its geographical mesoscale distribution;
- a better general aLMo QPF performance for larger precipitation intensities in terms of relative mean bias and standard deviation;

- consisteny of areal mean aLMo QPF error differences of 3 mm/24 h for classes 'high' and 'low' with a 1–1.5 K difference in the respective temperature biases as reported in the upper-air verification;
- substantially larger aLMo QPF errors for the southern side of the Alps (region 'TI') compared to the northern side (region 'SP');
- a number of systematically dry regions in the aLMo, best visible for class 'jet', the most prominent one being over the Swiss Plateau and the eastern flank of the Black Forest;
- a number of overly wet regions, strongly accentuated in cases of intensive precipitation, mostly related to orography.

The systematically dry and wet regions are likely to be related to incorrect description of the flow and the related production and transport of precipitation in vicinity of orography in the aLMo and may benefit from the prognostic precipitation scheme recently implemented.

The fact that the weather situation-dependent NWP model verification is able to discern and highlight specific model deficiencies offers, at the same time, a set of weather situations on which to test model developments and improvements.

The limitations of this study are related to the length of the data set not yielding large samples for every class. Moreover, the Schüepp weather classification is not specifically geared to precipitation and may, therefore, not be the optimal choice. Indeed, preliminary results using a subjective weather classification show consistent but clearer separation of weather situation-dependent aLMo QPF performance.

The SRN QPEs suffer from problems related to mountainous terrain, suboptimal performance of the La Dole radar in western Switzerland, and the relatively small domain it covers when compared to the aLMo domain. It is, therefore, very desirable to include radars of the neighbouring countries. A rough quantitative comparison with the precipitation verification over Switzerland done with the automatic station network (e.g. Schubiger 2002) reveals a large difference in the magnitude of the aLMo QPF overestimation when compared to the results shown in this study. One part of the difference can be attributed to the systematic underestimation of the SRN QPE, while another part may be due to the limited representativity of the precipitation point measurements in complex terrain delivered by the 69 Swiss automatic stations.

Next steps for this kind of analysis could be the inclusion of a precipitation analysis based on the high-resolution rain gauge network and the use of a more precipitation-geared weather classification. The application of a pattern matching method to identify systematic position errors (e.g. Rossa 2002) could be performed as a complement to the present analysis.

Acknowledgements

The authors gratefully acknowledge the expertise of Drs Jürg Joss and Urs Germann for direction on the careful use of the SRN QPEs, and Urs Germann for his comments on the manuscript.

References

Arpagaus, M., 2003. Verification of vertical profiles: Operational verification at MeteoSwiss This volume, ???–???.

Arpagaus, M., 2003. Upper-air verification at MeteoSwiss for 2002: Highlights. This volume, ???–???.

Damrath, U., 2002. Spatial distribution of precipitation over Germany and Switzerland. *COSMO Newsletter*, **2**, 72–74.

Doms, G., and U. Schättler, 1999. The nonhydrostatic limited-area model LM (Lokal-Modell) of DWD. Part I: Scientific documentation, http://www.cosmo-model.org.

Doms, G., A. Gassmann, E. Heise, M. Raschendorfer, C. Schraff, and R. Schrodin, 2001. Parameterization issues in the non-hydrostatic NWP-model LM. In: Key issues in the parameterization of subgrid physical processes, *ECMWF Seminar Proceedings, 3–7 September 2001*, 205–251.

Germann, U., and J. Joss, 2003. Operational measurement of precipitation in mountainous terrain. Chapter 2 in: Weather Radar: Principles and Advanced Applications (edited by P. Meischner), 2003, approx. 340 pp., to appear in *Springer monograph series "Physics of Earth and Space Environment"*.

Goeber, M., and S. Milton, 2002. On the use of radar data to verify Mesoscale Model precipitation forecasts. *Report of the SRNWP workshop on mesoscale verification 2001*, 18–27.

Joss, J., B. Schaedler, G. Galli, R. Cavalli, M. Boscacci, E. Held, G. Della Bruna, G. Kappenberger, V. Nespor, and R. Spiess, 1998. Operational use of radar for precipitation measurements in Switzerland, *Final Report of NRP 31. vdf Hochschulverlag an der ETH Zürich*, 108 pp., ISBN 3 7281 2501 6, http://vdf.ethz.ch.

Meischner, P., C. Collier, A. Illingworth, J. Joss, and W. Randeu, 1997. Advanced weather radar systems in Europe. *Bull. Amer. Meteor. Soc.*, **78**, 1411–1430.

Rossa, A. M., 2000. COST-717: Use of radar observations in hydrological and NWP models. *Physics and Chemistry of the Earth, Part B*, **10–12**, 1221–1224.

Rossa, A. M., 2002. Comparison of model and radar precipitation fields using a simple pattern matching method. *COSMO Newsletter*, **2**, 167–175.

Schubiger, F., 2002. Comparison of forecasts with and without nudging: Surface parameters over Switzerland for April – December 2001. *COSMO Newsletter*, **2**, 187–196.

Schüepp, M., 1979. Witterungsklimatologie, *Beiheft zu den Annalen der Schweizerischen Meteorologischen Anstalt (Jahrgang 1978)*, 1–93.

Schwarb, M., C. Daly, C. Frei, and C. Schär, 2001. Mittlere jährliche Niederschlagshöhen im europäischen Alpenraum 1971–1990. Sonderdruck aus: *Hydrologischer Atlas der Schweiz, 2001.*

Wanner, H., E. Salvisberg, R. Rickli, and M. Schüepp, 1998. 50 years of Alpine Weather Statistics (AWS), *Meteorol. Z.*, **N.F. 7**, 99–111.